Photodissociation of Yttrium and Lanthanum Oxide Cluster Cations

Z. D. Reed and M. A. Duncan*

Department of Chemistry, University of Georgia, Athens, Georgia 30602-2556

Received: January 21, 2008; Revised Manuscript Received: March 27, 2008

Transition metal oxide cations of the form $M_nO_m^+$ (M = Y, La) are produced by laser vaporization in a pulsed nozzle source and detected with time-of-flight mass spectrometry. Cluster oxides for each value of *n* form only a limited number of stoichiometries; $MO(M_2O_3)_x^+$ species are particularly intense. Cluster cations are mass selected and photodissociated using the third harmonic (355 nm) of a Nd:YAG laser. Multiphoton excitation is required to dissociate these clusters because of their strong bonding. Yttrium and lanthanum oxides exhibit different dissociation channels, but some common trends can be identified. Larger clusters for both metals undergo fission to make certain stable cation clusters, especially $MO(M_2O_3)_x^+$ species. Specific cations are identified to be especially stable because of their repeated production in the decomposition of larger clusters. These include $M_3O_4^+$, $M_5O_7^+$, $M_7O_{10}^+$, and $M_9O_{13}^+$, along with $Y_6O_8^+$. Density functional theory calculations were performed to investigate the relative stabilities and structures of these systems.

Introduction

Transition metal oxides have applications in electronics, ceramics, magnetic materials, and catalysis.[1–9] Their corresponding metal oxide nanoparticles expand the range of applications in magnetics, catalysis, and medicine.[10–16] Gas phase experiments on metal oxide clusters composed of fewer atoms (up to 50−60) have been investigated to model the stability, reactivity, and structure of solids and particles.[17–45] Many experiments have used mass spectrometry to probe these systems,[17–34] and some optical spectroscopy has been performed.[35–45] Theoretical calculations have examined the cage and network structures of oxide clusters, as well as their stabilities and spectra.[46–54] In the present work, we use time-of-flight mass spectrometry and mass-selected photodissociation measurements, along with density functional theory (DFT) calculations, to investigate the stability and structures of yttrium and lanthanum oxide cluster cations.

Mass spectrometry has been the standard method with which to investigate gas phase transition metal oxide clusters.[17–34] These experiments have most often used the relative intensities in the mass spectrum or patterns of reactivity to gauge relative cluster stability. Unlike the dramatic "magic numbers" seen for metal carbides,[55–61] a variety of stoichiometries are seen for transition metal oxide clusters. Castleman and co-workers have studied the mass spectrometry and collisional dissociation patterns of oxide clusters as well as their reactions with small hydrocarbons.[26] Bernstein and co-workers have used ultraviolet photoionization to study the mass spectra of these systems,[28] including yttrium oxide.[28] Our research group has employed mass spectrometry and mass selected photodissociation to a number of transition metal systems.[27] Matrix isolation[35] infrared and anion photoelectron techniques[36–42] have been used to examine the spectroscopy of certain small metal oxide molecules. Infrared resonance enhanced photodissociation (IR-REPD) in the far IR has been demonstrated to probe the vibrational spectroscopy of larger, more strongly bound clusters. Our group, along with Meijer and co-workers, has investigated metal oxide[43] and metal carbide[58] clusters using this technique. Other work on mass selected cations and anions has been performed by von Helden et al. and Asmis et al.[44,45] Theoretical calculations have been performed to gain information on the structures, stabilities, and spectra of various smaller metal oxide clusters to complement these experiments.[46–54]

The previous studies of metal oxide clusters[63,64] have revealed limitations and problems in the determination of relative cluster stabilities. The distribution of clusters produced in any experiment may be strongly influenced by the kind of source and the growth conditions, introducing possible biases toward larger or smaller clusters. Furthermore, some form of ionization is always necessary to detect clusters in mass spectrometers. Electron impact ionization and photoionization are both influenced by the unknown ionization potentials, size-dependent cross sections, and fragmentation processes. Variable energy collision induced dissociation (CID) has been used to fragment clusters to measure their dissociation energies,[33] but significant kinetic shifts, especially for strongly bound clusters, limit the accuracy of this technique. Variable energy photoabsorption experiments have been attempted for the same purpose, but absorption may not be efficient in the threshold region. Equilibrium mass spectrometry measurements have been performed for small vanadium oxide clusters,[17] and photofragmentation has been performed on bismuth and antimony oxides,[27a] and the vanadium group oxides,[27b] as well as the oxide clusters of chromium[27c] and iron.[27d] High energy atom bombardment has been used to study the metastable decay of lanthanum oxide.[24] In spite of these various studies, much uncertainty remains about which specific oxide clusters are stable, what causes the stability, and how the stoichiometries in stable clusters relate to those in known bulk oxide phases.

Our group has previously demonstrated that mass-selected photodissociation of metal compound cluster ions can be used to identify the stoichiometries that are the most stable.[27,56,65] These studies show that the stable cation clusters may or may not be prominent in the mass spectra of clusters produced initially by growth processes. However, stable cluster cations are resistant to decomposition, and they are likely to be produced more often on average than others in the fragmentation of larger clusters. Stable neutral clusters cannot be detected directly, but

* Corresponding author. Email: maduncan@uga.edu. Fax: 706-542-1234.

10.1021/jp800588r CCC: $40.75
Published on Web 05/22/2008

they can be inferred by mass conservation as the common leaving group in fragmentation processes. This photodissociation methodology has been used to study various metal carbides,[56] metal−silicon clusters,[65] and several metal-oxide cluster systems.[27] These studies have found trends in the dissociation behavior of these clusters and have identified a number of specific clusters of each type with special stability. In the case of oxides, we have found that stable species exhibit stoichiometries quite different from those that would be predicted on the basis of common metal oxidation states. Metal−oxygen ratios corresponding to less common bulk phases (e.g., FeO) are often formed in small clusters. Unlike the previously studied transition metals (V, Nb, Ta, Cr, Fe), which have several common oxidation states, yttrium and lanthanum, with valence configurations of $4d^15s^2$ and $5d^16s^2$, respectively, usually have only the +3 oxidation state in solid materials.[3] The mass spectrum of yttrium oxide has been studied by Bernstein et al.[28] and that of lanthanum oxide has been studied by Gibson[23] and Van Stipdonk et al.,[24] but photodissociation studies have not been applied to these systems. In the present work, we investigate the stabilities of yttrium oxide and lanthanum oxide clusters using photodissociation measurements along with density functional theory calculations.

Experimental Section

Metal oxide cluster ions are produced by laser vaporization in a pulsed nozzle source and mass analyzed in a reflectron time-of-flight spectrometer. This setup has been described previously.[27,56,65] The third harmonic (355 nm) of a Nd:YAG laser (Spectra Physics INDI-40) is employed to vaporize metal from the surface of a rotating and translating metal rod. Helium gas seeded with 1−10% oxygen is pulsed with a General Valve (60 psi backing pressure) through the sample rod holder, which has a 5 mm diameter bore and a 1 in. long growth channel. The metal oxide cluster cations grow directly in the laser-generated plasma and expand to form a molecular beam which is skimmed before it passes into a differentially pumped mass spectrometer chamber. A reflectron time-of-flight mass spectrometer with pulsed acceleration fields is used to sample the mass spectra of cation clusters produced under different conditions. To mass select specific clusters for photodissociation measurements, pulsed deflection plates are employed in the first flight tube section of the reflectron. Photoexcitation occurs in the turning region of the reflectron, where another Nd:YAG laser (Continuum SureLite) is timed to intersect the mass selected cation clusters. The parent ion and any fragment ions are mass analyzed in the second flight tube and are subsequently detected using an electron multiplier tube. The data are collected with a digital oscilloscope (Lecroy WaveRunner 342) and transferred to a PC computer using an IEEE-488 interface. Studies were performed at different fragmentation laser wavelengths (532 and 355 nm) and pulse energies (20−60 mJ/pulse over a roughly 1 cm^2 spot) to investigate the photodissociation mechanism.

To investigate the possible structures and energetics of these metal oxides, geometry optimizations were performed using density functional theory (DFT) computations with the Gaussian 03W program.[66] The Becke-3 Lee−Yang−Parr (B3LYP)[67,68] functional was used with the LANL2DZ basis set.[69–71] Atomization energies and energies per bond are reported for the minimum energy structures. No symmetry restrictions were placed on the clusters in the initial calculations, but those resulting structures that were close to symmetric were also investigated further with imposed symmetry. Theoretical investigations focused on the yttrium oxide clusters, with some

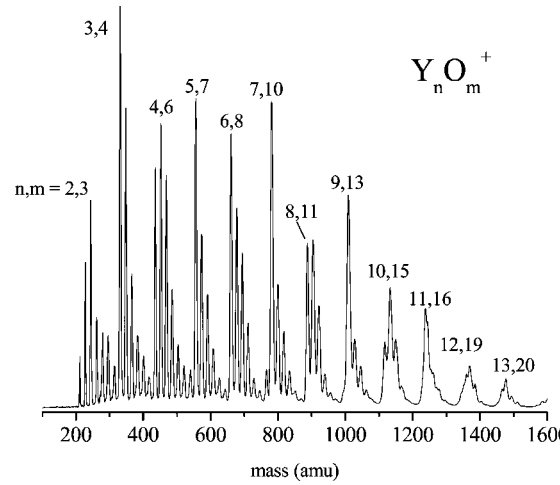

Figure 1. Time-of-flight mass spectrum for $Y_nO_m^+$ clusters formed in a He expansion with 5% O_2.

selected lanthanum oxide cluster calculations performed to investigate the possible differences between the two systems. Calculations were performed for YO, YO_2, YO_3, Y_2O_3, $Y_2O_3^+$, Y_3O_4, $Y_3O_4^+$, Y_4O_6, $Y_4O_6^+$, Y_5O_7, $Y_5O_7^+$, Y_6O_8, $Y_6O_8^+$, Y_7O_{10}, $Y_7O_{10}^+$, along with LaO, LaO_2, LaO_3, La_2O_3, $La_2O_3^+$, La_3O_4, $La_3O_4^+$, La_5O_7, and $La_5O_7^+$. The minimum energy structures, energies, and vibrational frequencies were computed for each cluster, and these data are reported in Supporting Information. Natural bond orbital (NBO) analysis, employing the Wiberg index,[66] was used to investigate the possible occurrence of metal−metal bonding across the oxide cage structures.

Results and Discussion

The mass spectrum of $Y_nO_m^+$ cation clusters produced is shown in Figure 1. As shown, oxide clusters are detected containing up to 13 or more metal atoms. The stoichiometries produced are not random. Instead, there is a strong tendency to form certain clusters preferentially. Species such as $Y_3O_4^+$, $Y_4O_6^+$, $Y_5O_7^+$, $Y_6O_8^+$, $Y_7O_{10}^+$, and $Y_9O_{13}^+$ are prominent. For convenience, these stoichiometries and others are designated as 3/4, 4/6, 5/7, and so forth, from here on. This mass spectrum changes slightly in its relative peak intensities with pulsed nozzle-vaporization laser timing and gas conditions, but the same prominent clusters are always observed. The number of oxygen atoms, *m*, is always greater than or equal to the number of metal atoms, *n*. Beyond that, many of the intense mass peaks fit the formula $YO(Y_2O_3)_x^+$, and it is apparent that these odd-numbered species are usually somewhat more abundant than the even-numbered species. Little change in stoichiometry is observed upon changing the oxygen concentration. The mass spectrum in Figure 1 is obtained with 5% O_2; the overall signals decrease with lower oxygen concentration, but values down to about 1% still produce spectra with comparable overall intensities. The oxygen concentration has a small effect on the stoichiometry of the $n = 4$ clusters, with $Y_4O_5^+$ (i.e., 4/5) the most prominent species at lower oxygen concentrations and 4/6 slightly more abundant at 5% oxygen or higher. The mass spectrum reported here is similar to the one reported by Bernstein and Kang using photoionization of neutral clusters,[28f] although no preference was apparent in their work for the odd numbered species.

The mass spectrum of $La_nO_m^+$ cation clusters can be seen in Figure 2, where clusters containing up to about 15 metal atoms are detected. Many stoichiometries similar to those seen for yttrium oxide are again found here; however, the preference to

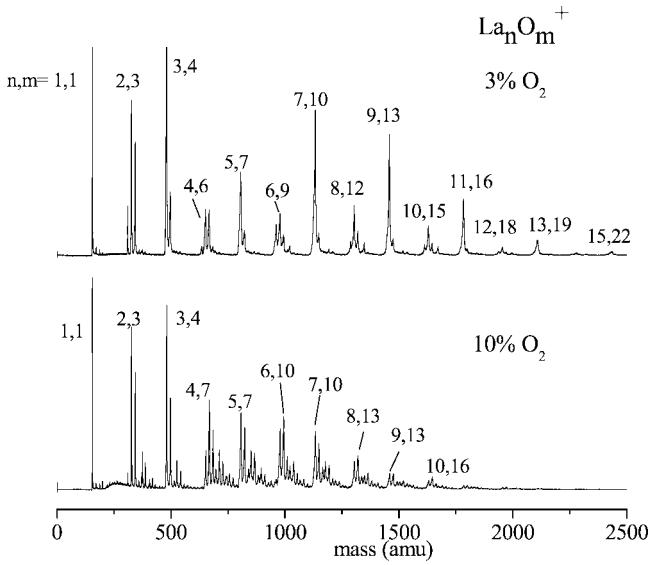

Figure 2. Time-of-flight mass spectra for $La_nO_m^+$ clusters formed in a He expansion with 3% (top) versus 10% (bottom) O_2 concentration.

form $LaO(La_2O_3)_x^+$ clusters appears to be stronger. The mass spectrum in the top pane of Figure 2 is obtained with a 3% oxygen gas mixture. The strong preference for odd numbered cation clusters is apparent, and all of the prominent species fit the $LaO(La_2O_3)_x^+$ stoichiometry. In the small clusters, the 3/4 species stands out, while in the larger clusters 7/10 and 9/13 are prominent. The 7/10 cluster has 3−4 times the intensity of its 6/9 or 8/12 neighbors, and it is also appreciably more intense than the 5/7 cation. At each metal atom increment, there is a limited number of oxide stoichiometries present, with some small intensity seen for the cation clusters containing only one oxygen more or less than the main cluster in that group. The two largest clusters observed, 13/19 and 15/22, both fit the $LaO(La_2O_3)_x^+$ stoichiometry and have no adjacent peaks with other amounts of oxygen. The bottom pane of Figure 2 shows the mass spectrum measured with a 10% oxygen gas mixture. Here, a wider variety of cluster cations are observed, with some metal sizes having up to eight more oxygen atoms than the most prominent cluster stoichiometry. In the $n = 4$ group, the 4/7 species is larger with 10% oxygen, but the 4/6 and 4/7 species have comparable intensities with 3% oxygen. There is also a slight preference for 8/13 with 10% oxygen instead of the 8/12 observed with 3% oxygen. These results generally agree with those seen by Gibson[23] and by van Stipdonk and co-workers,[24] although both of these previous studies detected primarily the major $LaO(La_2O_3)_x^+$ peaks and little else. It is not obvious why the lanthanide species vary more with the oxygen concentration or why they exhibit a stronger preference for the $MO(M_2O_3)_n^+$ stoichiometry. The growth conditions are the same for these species, and their bonding energetics are similar (see below). However, the clusters produced in experiments such as these have likely undergone many addition/fragmentation steps in growth, in addition to ionization/neutralization processes in the plasma. The energy deposited into the plasma may vary substantially because of the different species present and their detailed states, spectra, and energy transfer processes. Any further conclusions about the mass spectral intensities would therefore be highly speculative.

To investigate the relative stabilities of these clusters, we perform mass-selected photoexcitation experiments. Cation cluster masses with sufficient intensity are selected and then photodissociated by laser excitation in the reflectron at either

TABLE 1: Stoichiometries of Yttrium Oxide Photofragments ($Y_nO_m^+ = n/m$) Detected Using 355 nm[a]

cation clusters	fragment ions
4/5	3/4
4/6	**1/1**, 2/2, 2/3, 3/4
4/7	3/4, 4/5, 4/6
5/7	3/4
6/9	3/4
7/10	**3/4**, 5/7, 6/8
8/11	**3/4,** 5/7, 6/8
9/13	**3/4,** 5/7, 6/8, 7/10

[a] When multiple fragments are produced, especially prominent channels are indicated in bold.

TABLE 2: Stoichiometries of Lanthanum Oxide Photofragments ($La_nO_m^+ = n/m$) Detected Using 355 nm[a]

cation cluster	fragment ions
4/5	3/4
4/6	3/4
4/7	3/4, 4/5
5/7	3/4
6/8	3/4, **5/7**
6/9	5/7
7/10	5/7
8/12	7/10
9/13	7/10
11/16	9/13

[a] When multiple fragments are produced, especially prominent channels are indicated in bold.

355 or 532 nm. The lists of yttrium and lanthanum oxide cation clusters studied and their photofragments are presented in Tables 1 and 2. We find that either 355 or 532 nm induces photofragmentation in some but not all yttrium oxide clusters. However, only 355 nm yields fragmentation in the lanthanum oxide species. Relatively high laser fluences (40−60 mJ/pulse) are necessary to give detectable fragmentation in either system. This indicates that multiple photon excitation is necessary to break bonds in these clusters, consistent with the conditions we have applied in the past to study other transition metal oxide species.[27] This suggests, as we suspect, that the bond energies in these systems are quite high. Armentrout and co-workers determined the dissociation energy for the yttrium oxide diatomic to be 7.14 eV using zero-kinetic-energy (ZEKE) photoelectron spectroscopy.[33d] Jackson and co-workers determined the dissociation energy for LaO to be 9.07 eV using CID.[34] Although DFT calculations like these are not expected to provide quantitative binding energies, the results of these calculations presented later indicate that the per-bond dissociation energies for many of the larger clusters are around 6 eV. It is therefore understandable that these larger oxide clusters would also have strong bonds, thus explaining why extreme laser conditions are required for photodissociation. Dissociation is never efficient, but 355 nm laser light produces the largest fragment yield here, and thus all data shown are using this wavelength. We cannot tell whether the greater efficiency at 355 nm is due to the larger photon energy or to an improved absorption at this shorter wavelength. At the extreme laser powers employed here, it is conceivable that multiple photon processes could lead to doubly charged photofragments, via photoionization of singly charged fragment ions. However, no such species are detected.

Another observation in these photodissociation experiments supports the exceptional bond strength in these systems. The dissociation efficiency depends not only on the laser intensity used for dissociation but also on the vaporization laser intensity.

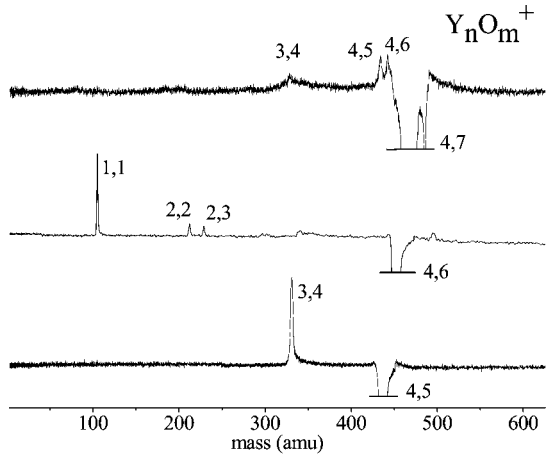

Figure 3. Photodissociation mass spectra for $Y_4O_m^+$ clusters at 355 nm. The parent ion depletion is marked as an off-scale negative-going peak.

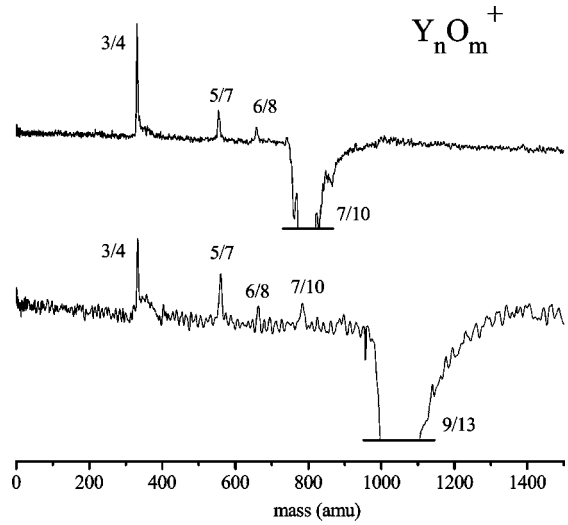

Figure 4. Photodissociation mass spectra for $Y_7O_{10}^+$ and $Y_9O_{13}^+$ clusters at 355 nm. The parent ion depletion is marked as an off-scale negative-going peak.

In the full mass spectra of both yttrium oxide and lanthanum oxide, little dependence on the vaporization laser was noticed other than a predictable decrease in signal when its power was too high or too low. However, upon mass selection, laser fluences of 15 mJ/pulse or greater lead to the production of signals for low-mass fragment peaks even without the photodissociation laser. These so-called metastable ion signals are familiar and are often seen with reflectron instruments when ions have significant internal energy. Even though we have collisional cooling via a supersonic expansion, the condensation energy from the formation of multiple metal oxide bonds, and perhaps the energy deposited into the metal-containing plasma upon vaporization, is too great to be cooled by collisions with the helium collision gas. Because of this unquenched internal energy, some prompt fragmentation likely occurs in the cluster source itself or in the transit time to the mass spectrometer, and we only detect the remnant of the internal energy which is still present at the mass spectrometer sampling position about 200 μsec downstream. For metastable ions to be detected, fragmentation must occur in the time window between the ion acceleration at this point and the reflectron turning region, which is an additional 60−80 μsec away from the source, depending on the mass. Such slow unimolecular dissociation like this is typically found only for strongly bound ions. Reducing the vaporization laser power eliminates the metastable fragmentation, presumably because clusters are not produced with as much internal energy. However, too much reduction in the vaporization laser intensity makes the photodissociation more difficult. We find that vaporization laser pulse energies of about 12 mJ/pulse were required to observe detectable photodissociation, regardless of the fragmentation laser pulse energy. This suggests that residual internal energy from the cluster formation process is needed to aid in the photofragmentation process. In the reflectron configuration that we use, photodissociation must occur on a time scale of 1−3 μsec to be detected. Apparently, the internal energy that these oxide clusters retain from their growth plus that imparted by photoexcitation makes it possible for the dissociation to occur within this time frame.

Figures 3 and 4 show typical photodissociation mass spectra for selected yttrium oxide clusters. These are shown in a difference mode, in which the mass spectrum with the fragmentation laser off is subtracted from that with it on. This gives a negative parent ion peak indicating its depletion and positive fragment peaks. In an ideal scenario, the integrated fragment peak intensities would equal the amount of depletion. However, mass discrimination in this photodissociation configuration makes it difficult to focus simultaneously on parent ions and their fragments.[72] We can therefore distinguish between strong and weak fragmentation channels but cannot give any quantitative branching ratios. In the present experiments, the fragmentation yield is so extremely small that the fragment signal often cannot be seen shot-by-shot on the oscilloscope, making it difficult to focus on these species. The parent ion is always at least partially focused, and its depletion is therefore more intense. It is conceivable that fragment ion detection is affected by some translational energy release in these photofragments, but this is not generally expected to be prominent in multiphoton processes, which deposit energy nonspecifically into many internal states. In each of the fragmentation spectra here, the parent ion depletion is offscale, and its intensity is therefore limited with a horizontal line.

Figure 3 shows a series of $n = 4$ cluster cations and their fragments. This group of clusters showed no clear stoichiometric preference in the mass spectrum, with the most intense cluster in the group depending on the oxygen concentration. The 4/5 cluster has a relatively efficient fragmentation to form the 3/4 species. The 4/6 species fragments to produce the smaller 2/2, 2/3, and 1/1 ions. This cluster is the only one that leads to such small fragments. The 4/7 cation fragments to produce 4/6 and 4/5 by losing one or two oxygen atoms, and also to a small amount of 3/4. The fragmentation from 4/7 → 4/6 must occur by loss of atomic oxygen, while the production of 4/5 could occur by the loss of either two atoms or the O_2 molecule. Likewise, the production of the 3/4 charged fragment here could be accompanied by atomic or molecular neutrals. Unfortunately in this case and others below, we cannot identify the missing neutral(s) which would elucidate whether the mechanism of decomposition is sequential or concerted. We therefore indicate neutral losses in brackets, e.g. [O_2], to emphasize this uncertainty. It is also true that we cannot distinguish between concerted and sequential fragmentation processes. The fragment ions seen here could be formed stepwise or all in parallel. Laser power dependence does not reveal any change in relative ion intensities, but this is not a definitive way to identify the mechanism. Therefore, we focus on just the nature of the fragments formed and the neutral losses that must go along with these.

Figure 4 shows the fragmentation mass spectra for the $Y_7O_{10}^+$ and $Y_9O_{13}^+$ clusters. The 7/10 species fragments to form 6/8, 5/7, and 3/4, with the 3/4 ion the most intense. Each of these fragments are immediately recognizable as the most intense stoichiometries seen in the mass spectrum coming out of the cluster source. The 9/13 cluster fragments to produce 7/10, and then the rest of the smaller fragment ions are the same for both parents. As noted above, we cannot determine what the specific neutral fragments are that go along with these ions. In every case, atomic or molecular neutral species are possible that would conserve mass. However, it is interesting to note the repeated occurrence of the 2/3 interval in the neutrals. Except for the 6/8 species, there is a common interval of 2/3 for the apparent sequence 9/13 → 7/10 → 5/7 → 3/4. Y_2O_3 is of course the stoichiometry of the most common bulk oxide of yttrium.[1–3]

These selected fragmentation mass spectra in Figures 3 and 4 already demonstrate the features common to all of the yttrium oxide clusters that we have studied, as listed in Table 1. The 3/4, 5/7, 6/8, and 7/10 ions are produced many times from many parent ion dissociation processes. Except for the 6/8 species, these all have an odd number of metal atoms and fit the general formula of $YO(Y_2O_3)_n^+$, where $n = 1, 2, 3$. Except for the formation of the 6/8 species, these ions often fragment by the loss of the [2/3] neutral interval or some multiple of this. It is therefore tempting to view their fragmentation as a sequential loss of the [2/3] neutral. Other ions that we have selected that are not one of these $YO(Y_2O_3)_n^+$ species tend to lose whatever group is necessary to produce one of these ions. The only even-numbered ion that is produced in multiple fragmentation events is 6/8. There are no prominent two, four, or eight-atom fragment ions.

Lanthanum oxide clusters fragment in much the same way that the yttrium species do. Here, fragmentation is extremely inefficient, even compared with the yttrium oxide systems. The fragmentation data shown was averaged for considerably longer than the yttrium oxide data and still shows very low signals. The fragmentation channels for each mass selected cation cluster are shown in Table 2. Photofragmentation was attempted with both 355 and 532 nm, but fragmentation was only observed with 355 nm. Although different distributions of lanthanum oxide clusters are observed when the oxygen concentration is varied, there are no differences in the fragmentation channels observed when the same parent ion is studied.

Figure 5 shows the photofragmentation data for the 4/6 and 4/7 clusters. In the top frame, the fragmentation of 4/7 produces the 4/5 and 3/4 species. Again, the possible paths to 4/5 are via the loss of O_2 or two oxygen atoms. Unlike in yttrium oxide, no channel is observed for the loss of a single oxygen atom, suggesting that the 4/7 → 4/5 process occurs by the loss of O_2. The 3/4 fragment could be formed by a single loss of neutral [1/3] or by a sequential loss of [O_2] and then [1/1]. The latter seems more likely, as the [1/3] neutral should not be as stable as [1/1] because of the likely oxidation state of the metal. Theory was performed to investigate this, as discussed below. In the lower frame, the dissociation of the 4/6 species to produce 3/4 indicates a neutral loss of [1/2].

Figure 6 shows the photofragmentation data for several other representative $La_nO_m^+$ clusters, chosen mainly by their availability with good intensity in the mass spectrum from the source. The top trace shows the fragmentation of 9/13, which produces the next smaller $LaO(La_2O_3)_x$ cation, 7/10, with a neutral difference of [2/3]. The middle trace shows the fragmentation of 7/10, which again loses [2/3] to yield 5/7, which is another $LaO(La_2O_3)_x^+$ cluster. Most of the other clusters are also found

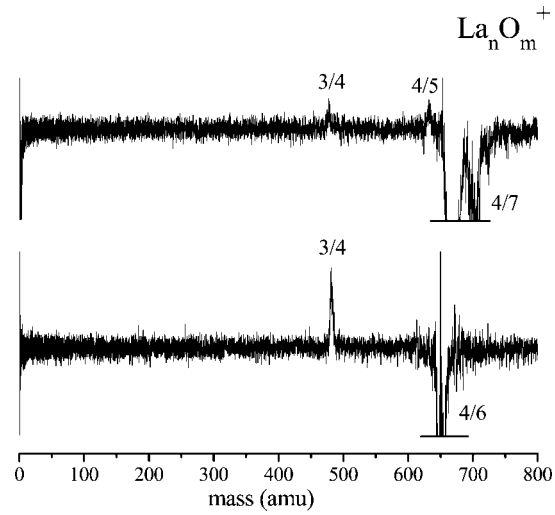

Figure 5. Photodissociation mass spectra for $La_4O_m^+$ clusters at 355 nm. The parent ion depletion is marked as an off-scale negative-going peak.

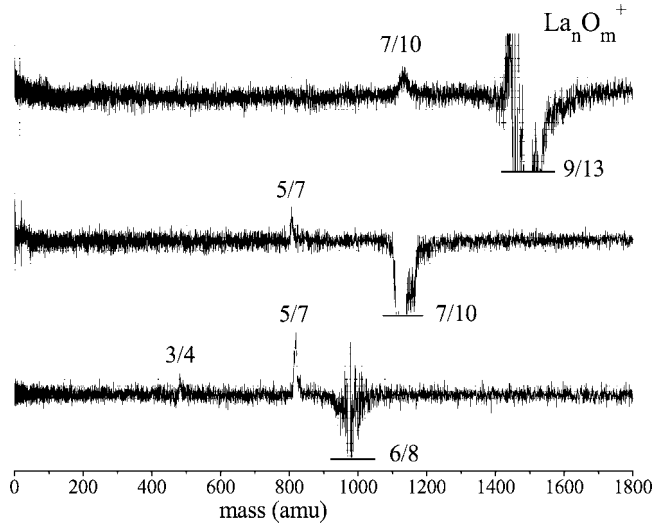

Figure 6. Photodissociation mass spectra for $La_6O_8^+$, $La_7O_{10}^+$, and $La_9O_{13}^+$ clusters at 355 nm. The parent ion depletion is marked as an off-scale negative-going peak.

to fragment in this way, eliminating [2/3] to form the next smallest $LaO(La_2O_3)_x$ cation cluster. The main exception to this pattern is the 6/8 species, whose fragmentation is shown in the lower trace. The charged fragments here are 5/7 and 3/4, implying that 6/8 loses [1/1] and then the 5/7 species produced fragments in exactly the way the selected 5/7 ion does, by the elimination of [2/3] to produce 3/4. The 6/9 cluster (not shown) has a single fragmentation channel to produce 5/7, implying the loss of [1/2].

The fragmentation in all of these lanthanum oxide clusters seems to be driven by the strong tendency to form the $LaO(La_2O_3)_x^+$ stoichiometry. Other fragmentation channels are rare and only observed for the clusters which are less intense in the mass spectrum. When the $LaO(La_2O_3)_x$ cation clusters fragment, they all lose units of neutral [2/3], which is the bulk stoichiometry. Van Stipdonk and co-workers observed similar behavior in the metastable decay of $LaO(La_2O_3)_x^+$ clusters.[24] These particular clusters demonstrate considerably less efficient photofragmentation compared with the even numbered clusters. Given the dramatic preference for these clusters in the mass spectrum and how they dominate the fragmentation channels,

it seems likely that they are significantly more stable than other cluster stoichiometries.

Some insight can be gained from comparing these yttrium and lanthanum oxides. Both have the same bulk stoichiometries, M_2O_3. In the mass spectra for both systems, the $MO(M_2O_3)_x^+$ cations are more intense than the clusters with even numbers of metal atoms. For these odd-numbered metal species, there is little variation in the number of oxygen atoms. This is not the case for the even-numbered clusters, which demonstrate no clear preference for a specific number of oxygens. In the fragmentation processes of both yttrium and lanthanum oxides, $MO(M_2O_3)_x$ cations are universally the most abundant, as is the loss of neutral [2/3]. For the even-numbered ions of both metals, the initial neutral loss varies as needed to produce the nearest $MO(M_2O_3)_x^+$ species as the highest mass charged fragment. Smaller fragments then follow the same $MO(M_2O_3)_x^+$ sequence seen for the other clusters. This indicates that the production of $MO(M_2O_3)_x$ cations is the strongest driving force behind these fragmentation processes. Another important tendency is the loss of the [2/3] neutral unit.

The similarities between these yttrium and lanthanum systems are striking, but there are also differences. In particular, the overall fragmentation processes for lanthanum are less efficient than those for yttrium, and fewer fragment channels are detected for lanthanum. This is consistent with a sequential fragmentation mechanism for both kinds of systems, which proceeds to a greater extent for the yttrium species. This suggests that the bond energies for the yttrium species are generally lower than those for the lanthanum species. The most common step in the sequential fragmentation appears to be the elimination of the [2/3] neutral corresponding to the bulk stoichiometry. Another noticeable difference is the importance of the 6/8 cluster for the yttrium oxides. This is a prominent species in the mass spectrum of the clusters produced by the source, and it is the only cluster with an even number of metal atoms produced as a common fragment ion. This particular cluster appears to be quite important for yttrium oxides, but not for lanthanum.

The stoichiometries seen in these yttrium and lanthanum oxide clusters are reasonable in light of the metal oxidation states known for these metals. As noted, both lanthanum and yttrium oxides take the form M_2O_3 in the bulk, where the metal oxidation state is +3. If we average over all of the atoms without regard to structural arrangements, the $MO(M_2O_3)_x^+$ cations seen throughout the data here for both metals indicate that the metal in these clusters has the same +3 oxidation state. This same $MO(M_2O_3)_x^+$ stoichiometry was observed previously for oxide clusters of aluminum[35c] and those of antimony and bismuth,[27a] where the +3 oxidation state is also expected. Apparently, this stoichiometry pattern is the best way for these clusters to maintain the +3 oxidation state while accommodating the single positive charge. Yttrium is also known to have a +2 oxidation state in metal hydrides, as does lanthanum in hydrides, sulfides, tellurides and selenides.[3] The 1/1 neutral seen occasionally in the data here as a leaving group can be rationalized in this way, along with the 4/5 and 6/8 clusters, which would require a single metal atom in this lower oxidation state. However, there is no simple way to assign common oxidation states to some of the other even numbered metal clusters produced as minor species in the source distribution. At least one metal with a +4 oxidation state would be necessary in the 4/6, 6/9, and 8/12 clusters. Although some of these latter species deviate from this, it is clear that the most stable species produced for both of these metals follow the $MO(M_2O_3)_x^+$ formula and have the most common +3 oxidation state. This behavior is quite different from that seen previously for other transition metals. In our studies of the vanadium group (V, Nb, Ta) oxides, where the normal oxidation state is +5, we found evidence for lower oxidation states (average values of 4.5) in the smaller clusters.[27b] In the case of chromium oxides, where the most common oxidation state is +3 (as in Cr_2O_3), the small clusters preferred the higher +6 oxidation state, which is known, but less common, for chromium (as in CrO_3).[27c] In the iron system, the small clusters preferred the +2 oxidation state and 1:1 oxide stoichiometries rather than the more common +3 value seen in Fe_2O_3.[27d] Thus, we have seen significant variation in the oxidation states of small transition metal oxides compared with the most common bulk phases in other studies. However, the yttrium and lanthanum systems seen here follow the same oxidation state trend seen in the most common solids.

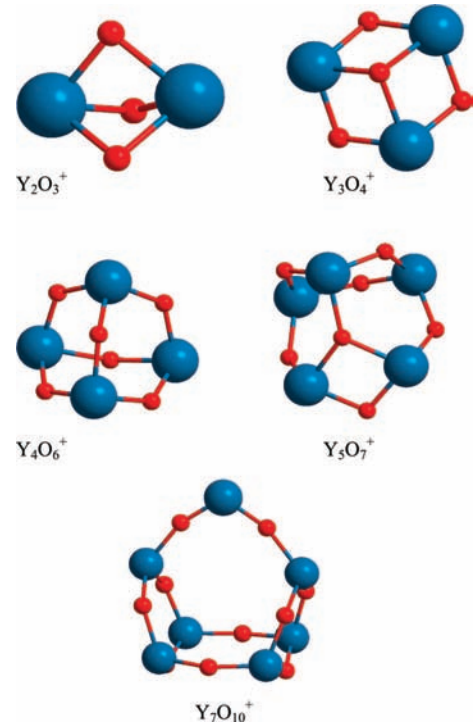

Figure 7. Structures computed for various Y_nO_m clusters.

To further investigate the stability of the specific ions and neutrals identified here, we performed DFT calculations to find the lowest energy structure and binding energies, using the B3LYP functional. The prominent cations $Y_2O_3^+$, $Y_3O_4^+$, $Y_4O_6^+$, $Y_5O_7^+$, $Y_6O_8^+$, and $Y_7O_{10}^+$ were investigated. Additionally, the possible neutral leaving groups YO, YO_2, YO_3, and Y_2O_3 were investigated. To investigate possible differences in structure between lanthanum oxide and yttrium oxide, selected lanthanum oxide clusters were also included in these computational studies (La_2O_3, $La_2O_3^+$, La_3O_4, $La_3O_4^+$, La_5O_7, and $La_5O_7^+$). The schematic minimum energy structures found for these clusters are shown in Figure 7 and Figure 8. The cations and neutrals have quite similar structures, only differing slightly in bond lengths and angles. In these figures, only one structure for each stoichiometry is shown; additional details are presented in Supporting Information along with the calculated vibrational frequencies. For each of the stable cations, the corresponding neutral was investigated to explore the role of charge on the relative stability. The energetics for these systems are summarized in Table 3 and Table 4. For each cluster studied, numerous starting geometries and spin states were investigated in the search to locate the most likely structures for these species.

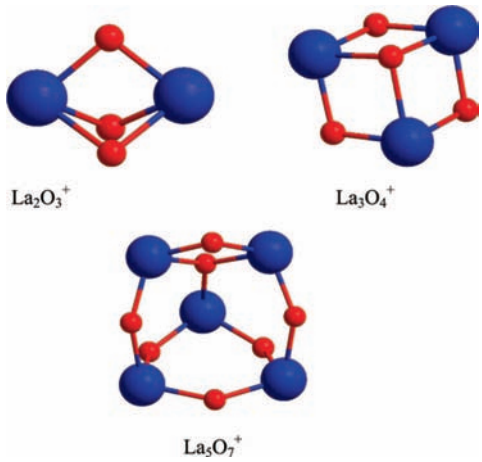

Figure 8. Structures computed for various La_nO_m clusters.

TABLE 3: Energies Computed Using B3LYP for the Yttrium Oxide Clusters Studied Here[a]

	atomization energy	energy per bond	ground state
YO	154.8	154.8	$^2\Sigma$
YO_2	235.6	117.8	$^2\Sigma_u$
Y_2O_3	815.3	135.6	^1A
$Y_2O_3^+$	819.5	136.6	^2A
Y_3O_4	1175.6	130.6	^2A
$Y_3O_4^+$	1248.9	138.8	^1A
Y_4O_6	1789.1	149.1	^1A
$Y_4O_6^+$	1790.9	149.2	^2A
Y_5O_7	2126.0	141.7	^2A
$Y_5O_7^+$	2200.1	146.7	^1A
Y_7O_{10}	3036.5	151.8	^2A
$Y_7O_{10}^+$	3101.9	155.1	^1A

[a] All units are kilocalories per mole.

TABLE 4: Energies Computed Using B3LYP for the Lanthanum Oxide Clusters Studied Here[a]

	atomization energy	energy per bond	ground state
LaO	229.1	229.1	$^2\Sigma$
LaO_2	400.9	200.5	$^2\Sigma_u$
La_2O_3	652.1	108.7	^1A
$La_2O_3^+$	795.6	132.6	^2A
La_3O_4	1153.0	128.1	^2A
$La_3O_4^+$	1210.4	134.5	^1A
La_5O_7	2064.1	137.6	^2A
$La_5O_7^+$	2130.0	142.0	^1A

[a] All units are kcal/mol.

Unfortunately, none of even the diatomic or triatomic species here have been studied with high resolution spectroscopy whereby we could test ground-state bond distances or spin configurations.

As shown in Figure 7 and Figure 8, the structures for these oxides are cage-like with alternating metal−oxygen−metal bonds. Each oxygen is bonded to two or three metal atoms and each metal forms at least three bonds, consistent with the +3 oxidation state. There are no terminal oxygens; that is, oxygen atoms only attached to a single metal via a double bond. Terminal oxygens like this have been seen in the structures of all previous transition metal oxide systems that we have studied (V, Nb, Ta, Cr) except iron[27] and are the result of higher metal oxidation states. No internal atoms are found for any of these clusters. NBO analysis shows that all of the bonding occurs along the edges of these structures, with no significant metal−metal interactions across the interior of the cages. Lanthanum oxide clusters are calculated to have the same general structures as the corresponding yttrium species, but the bond distances are generally longer. For each stoichiometry, the neutral and cation have essentially the same structure, with only minor differences in bond lengths and angles. These structures presumably maximize the number of strong metal−oxygen bonds. Interestingly, the structures shown here for the smaller clusters are pretty much the same as those we proposed several years ago in our study of antimony and bismuth oxide clusters.[27a] At that time, we were not able to do any DFT calculations, but instead just used the expected oxidation states and connected the atoms to make structures that satisfied their bonding capacity. It is satisfying that the more sophisticated DFT calculations here arrive at the same qualitative conclusions for these structures. The NBO analysis also provides a charge on each atom, which is within ±0.2 of +3 for each metal atom and −2 for each oxygen, consistent with the expected ionic bonding.

The bond energies in these clusters are all quite high, as is typical for metal oxides. Table 3 shows that the per bond dissociation energy varies from 59 to 155 kcal/mol (2.56 to 6.72 eV) for yttrium oxide, with the larger clusters having bond energies around 150 kcal/mol (6.5 eV). Lanthanum oxide clusters (Table 4) have per bond energies ranging from 100 to 142 kcal/mol (4.3−6.2 eV), with the larger clusters again having bond energies around 140 kcal/mol (6.1 eV). These bond energies are significantly greater than those for other transition metal oxides that we have studied.[27] For example, the per-bond energy computed for chromium oxide clusters with the same DFT methods were in the range of 70−90 kcal/mol.[27c] DFT is of course not reliable for quantitative energetics in clusters of this type, but the relative energies computed indicate that the yttrium and lanthanum clusters are quite strongly bound. We can investigate the effect of charge on bonding energetics as well. The atomization energies are relative to separated neutral atoms or to separated neutrals and one metal ion, respectively. By using this as a reference, the cations here are found to be slightly more stable than the corresponding neutrals. It is possible in principle to use the difference in atomization energies for neutrals and ions to derive ionization potentials for the neutral clusters. However, because DFT energetics are not quantitative even for the atomic metal species, such an exercise would not be useful. Although the atomization energy is generally higher for yttrium oxide, the lanthanum oxide clusters proved to be more difficult to fragment and had fewer fragmentation channels. However, the absorption cross sections for lanthanum and yttrium oxide are unknown, so lanthanum oxide may simply not absorb light at the wavelengths used as efficiently as yttrium oxide.

The calculated energetics prove somewhat useful in explaining the observed stabilities and fragmentation patterns. YO and YO_2 are strongly bound, but YO_3 does not converge to a stable structure. This suggests that the loss of [1,3] in our photodissociation experiments most likely represents the simultaneous, or rapid sequential, loss of YO and O_2. The same is seen with lanthanum clusters, where LaO_3 does not converge to a stable structure. The computed atomization energy for YO (6.71 eV) is somewhat lower than the value measured by Armentrout et al. (7.14 eV).[33d] The computed value for LaO (9.93 eV) compares somewhat less favorably to Jackson's measured value of 9.07 eV.[34] Although these comparisons are reasonable, some of the energetics computed for the larger clusters are somewhat troubling. Oddly, both the Y_4O_6 cation and the Y_4O_6 neutral are calculated to be among the most stable clusters per bond, but these are not seen as fragments in any case other than the dissociation of 4/7. $Y_3O_4^+$ and the Y_2O_3 are not calculated to

be especially stable relative to other clusters, but these are seen to be the most intense cation fragment and the most common neutral leaving group, respectively, throughout our data. Y_2O_3 is not calculated to be more stable than the cation, despite having the same stoichiometry as bulk yttrium oxide. On the other hand, the Y_7O_{10} cation is nearly 20 kcal/mol more stable per bond than the 5/7 cation; this species is quite prominent in the mass spectrum, and it appears in the fragmentation of all clusters with $n > 7$.

Another trend running through the data for both metal oxide systems is that the per-bond dissociation energies increase with cluster size. The 5/7 clusters for both metals have energies of about 140 kcal/mol, while the 7/10 value for yttrium is about 150 kcal/mol. These are significantly greater than the 2/3 and 3/4 values for both metals. Apparently, the smaller cage structures are strained compared with the larger ones. It could then be speculated that the smaller cage species here are more reactive than their larger cage counterparts. Reaction kinetics studies on these systems would therefore be interesting to test this possibility.

Conclusions

Yttrium and lanthanum oxide clusters produced by laser vaporization have been investigated with time-of-flight mass spectrometry and mass-selected photodissociation. Only a limited number of oxide stoichiometries are observed for each cluster size. There is a strong preference for odd numbered metal clusters in the mass spectrum. Dissociation produces mainly the same ions, most commonly those with the $MO(M_2O_3)_x^+$ stoichiometry. Yttrium oxide clusters are observed to have a variety of fragmentation channels. Photodissociation appears to be a sequential process, with the loss of the M_2O_3 neutral occurring throughout the data for both metals. In addition to the $MO(M_2O_3)_x^+$ ions and M_2O_3 neutrals, the $Y_6O_8^+$ cluster is also formed prominently by cluster growth and is a common photofragment. Lanthanum oxide clusters rarely have more than one fragmentation channel, with $LaO(La_2O_3)_x^+$ fragments produced almost exclusively. Unlike other transition metal oxide clusters studied previously, the +3 oxidation state implied by the data here for both of these cluster systems is exactly the same as that for the corresponding bulk oxides.

Density functional theory computations on these clusters produce structures that are visually and geometrically appealing, which lead to high bonding stability. Examination of the per-bond energetics gives some insight into the stabilities of the clusters, but the picture is not as clear as in the experiment. Future theoretical investigations of these systems could be useful. These oxide systems have greater per-bond binding energies than many other transition metal oxide clusters. Because of this high intrinsic stability, these systems may be interesting for isolation in macroscopic quantities as nanocluster materials. Because several of these systems are closed-shell singlets with an overall single charge, they might be less reactive and produce more stable solids if co-condensed with negatively charged ligands.

Acknowledgment. We gratefully acknowledge generous support for this work from the Air Force Office of Scientific Research (Grant No. FA9550-06-1-0028).

Supporting Information Available: The full citation for ref66 as well as additional details for the density functional calculations on the clusters studied here. This material is available free of charge via the Internet at http://pubs.acs.org.

References and Notes

(1) Cox, P. A. *Transition Metal Oxides*; Clarendon Press: Oxford, 1992.
(2) Rao, C. N.; Raveau, B. *Transition Metal Oxides*; John Wiley: New York, 1998.
(3) Cotton, F. A.; Wilkinson, G.; Murillo, C. A.; Bochmann, M. *Advanced Inorganic Chemistry*, 6th ed.; John Wiley & Sons: New York, 1999.
(4) Hayashi, C.; Uyeda, R.; Tasaki, A. *Ultra-Fine Particles*; Noyes: Westwood, 1997.
(5) Henrich, V. E.; Cox, P. A. *The Surface Science of Metal Oxides*; Cambridge University Press: Cambridge, 1994.
(6) Somorjai, G. A. *Introduction to Surface Chemistry and Catalysis*; Wiley-Interscience: New York, 1994.
(7) Gates, B. C. *Chem. Rev.* **1995**, *95*, 511.
(8) (a) Rainer, D. R.; Goodman, D. W. *J. Mol. Catal. A: Chem.* **1998**, *131*, 259. (b) St. Clair, T. P.; Goodman, D. W. *Top. Catal.* **2000**, *13*, 5. (c) Wallace, W. T.; Min, B. K.; Goodman, D. W. *Top. Catal.* **2005**, *34*, 17. (d) Chen, M. S.; Goodman, D. W. *Acc. Chem. Res.* **2006**, *39*, 739.
(9) (a) Wachs, I. E.; Briand, L. E.; Jehng, J. M.; Burcham, L.; Gao, X. T. *Catal. Today* **2000**, *57*, 323. (b) Chen, Y. S.; Wachs, I. E. *J. Catal.* **2003**, *217*, 468. (c) Wachs, I. E. *Catal. Today* **2005**, *100*, 79. (d) Wachs, I. E.; Jehng, J. M.; Ueda, W. *J. Phys. Chem. B* **2005**, *109*, 2275. (e) Tian, H. J.; Ross, E. I.; Wachs, I. E. *J. Phys. Chem. B* **2006**, *110*, 9593.
(10) Pope, M. T; Müller, A. *Poloyoxometalate Chemistry From Topology via Self-Assembly to Applications*; Kluwer: Boston, 2001.
(11) Crans, D. C.; Smee, J. J.; Gaidamauskas, E.; Yang, L. Q. *Chem. Rev.* **2004**, *104*, 849.
(12) (a) Rockenberger, J.; Scher, E. C.; Alivisatos, A. P. *J. Am. Chem. Soc.* **1999**, *121*, 11595. (b) Puntes, V. F.; Krishnan, K. M.; Alivisatos, A. P. *Science* **2001**, *291*, 2115. (c) Nolting, F.; Luning, J.; Rockenberger, J.; Hu, J.; Alivisatos, A. P. *Surf. Rev. Lett.* **2002**, *9*, 437. (d) Jun, Y. W.; Casula, M. F.; Sim, J. H.; Kim, S. Y.; Cheon, J.; Alivisatos, A. P. *J. Am. Chem. Soc.* **2003**, *125*, 15981. (e) Casula, M. F.; Jun, Y. W.; Zaziski, D. J.; Chan, E. M.; Corrias, A.; Alivisatos, A. P. *J. Am. Chem. Soc.* **2006**, *128*, 1675.
(13) Ayers, T. M.; Fye, J. L.; Li, Q.; Duncan, M. A. *J. Cluster Sci.* **2003**, *14*, 97.
(14) Cushings, B. L.; Kolesnichenko, V. L.; O'Connor, C. J. *Chem. Rev.* **2004**, *104*, 3893.
(15) Fernandez-Garcia, M.; Martinez-Arias, A.; Hanson, J. C.; Rodriguez, J. A. *Chem. Rev.* **2004**, *104*, 4063.
(16) Stepanov, A. L.; Boura, G.; Gartza, M.; Osinb, Y. N.; Reinholdta, A.; Kreibig, U. *Vacuum* **2004**, *64*, 9.
(17) (a) Berkowitz, J.; Chupka, W. A.; Inghram, M. G. *J. Chem. Phys.* **1957**, *27*, 87. (b) Inghram, M. G.; Chupka, W. A.; Berkowitz, J. *J. Chem. Phys.* **1957**, *27*, 569.
(18) Farber, M.; Uy, O. M.; Srivastava, R. D. *J. Chem. Phys.* **1972**, *56*, 512.
(19) Bennett, S. L.; Lin, S. S.; Gilles, P. W. *J. Phys. Chem.* **1974**, *78*, 266.
(20) Kahwa, I. A.; Selbin, J. *Inorg. Chim. Acta* **1988**, *144*, 275.
(21) Knickelbein, M. *J. Chem. Phys.* **1995**, *102*, 1.
(22) Knickelbein, M. *Phys. Rev. B* **2005**, *71*, 1.
(23) Gibson, J. K. *J. Appl. Phys.* **1995**, *78*, 1274.
(24) (a) Van Stipdonk, M. J.; Schweikert, E. A. *Nuclear Instruments and Methods in Physics Research B* **1995**, *96*, 530. (b) Van Stipdonk, M. J.; Justes, D. R.; English, R. D.; Schweikert, E. A. *J. Mass Spectrom.* **1999**, *34*, 677.
(25) (a) Kooi, S. E.; Castleman, A. W. *J. Phys. Chem. A* **1999**, *103*, 5671. (b) Bell, R. C.; Zemski, K. A.; Justes, D. R.; Castleman, A. W. *J. Chem. Phys.* **2001**, *114*, 798.
(26) (a) Deng, H. T.; Kerns, K. P.; Castleman, A. W. *J. Phys. Chem.* **1996**, *100*, 13386. (b) Bell, R. C.; Zemski, K. A.; Kerns, K. P.; Deng, H. T.; Castleman, A. W. *J. Phys. Chem. A* **1998**, *102*, 1733. (c) Bell, R. C.; Zemski, K. A.; Castleman, A. W. *J. Cluster Sci.* **1999**, *10*, 509. (d) Zemski, K. A.; Justes, D. R.; Castleman, A. W. *J. Phys. Chem. B* **2002**, *106*, 6136. (e) Justes, D. R.; Mitric, R.; Moore, N. A.; Bonacic-Koutecky, V.; Castleman, A. W. *J. Am. Chem. Soc.* **2003**, *125*, 6289. (f) Justes, D. R.; Moore, N. A.; Castleman, A. W. *J. Phys. Chem. B* **2004**, *108*, 3855. (g) Bergeron, D. E.; Castleman, A. W.; Jones, N. O.; Khanna, S. N. *Nano. Lett.* **2004**, *4*, 261. (h) Moore, N. A.; Mitric, R.; Justes, D. R.; Bonacic-Koutecky, V.; Castleman, A. W. *J. Phys. Chem. B* **2006**, *110*, 3015. (i) Reilly, N. M.; Reveles, J. U.; Johnson, G. E.; Khanna, S. N.; Castleman, A. W. *Chem. Phys. Lett.* **2007**, *435*, 295.
(27) (a) France, M. R.; Buchanan, J. W.; Robinson, J. C.; Pullins, S. H.; Tucker, J. L.; King, R. B.; Duncan, M. A. *J. Phys. Chem. A* **1997**, *101*, 6214. (b) Molek, K. S.; Jaeger, T. D.; Duncan, M. A. *J. Chem. Phys.* **2005**, 123. (c) Molek, K. S.; Reed, Z. D.; Ricks, A. M.; Duncan, M. A. *J. Phys. Chem. A* **2007**, *111*, 8080. (d) Molek, K. S.; Anfuso, C.; Duncan, M. A. *J. Phys. Chem. A.* in press.
(28) (a) Foltin, M.; Stueber, G. J.; Bernstein, E. R. *J. Chem. Phys.* **1999**, *111*, 9577. (b) Shin, D. N.; Matsuda, Y.; Bernstein, E. R. *J. Chem. Phys.* **2004**, *120*, 4150. (c) Shin, D. N.; Matsuda, Y.; Bernstein, E. R. *J. Chem.*

Phys. **2004**, *120*, 4157. (d) Matsuda, Y.; Bernstein, E. R. *J. Phys. Chem. A* **2005**, *109*, 314. (e) Matsuda, Y.; Bernstein, E. R. *J. Phys. Chem. A* **2005**, *109*, 3803. (f) Kang, Y.; Bernstein, E. R. *Bull. Korean Chem. Soc.* **2005**, *26*, 345. (g) Dong, F.; Heinbuch, S.; He, S. G.; Xie, Y.; Rocca, J. J.; Bernstein, E. R. *J. Chem. Phys.* **2006**, *125*, 164318.

(29) (a) Harvey, J. N.; Diefenbach, M.; Schröder, D.; Schwarz, H. *Int. J. Mass. Spectrom.* **1999**, *183*, 85. (b) Schröder, D.; Schwarz, H.; Shaik, S. *Struct. & Bonding* **2000**, *97*, 91. (c) Jackson, P.; Fisher, K. J.; Willett, G. D. *Chem. Phys.* **2000**, *262*, 179. (d) Jackson, P.; Harvey, J. N.; Schröder, D.; Schwarz, H. *Int. J. Mass. Spectrom.* **2001**, *204*, 233. (e) Schröder, D.; Engeser, M.; Schwarz, H.; Harvey, J. N. *ChemPhysChem* **2002**, *3*, 584. (f) Koszinowski, K.; Schlangen, M.; Schröder, D.; Schwarz, H. *Eur. J. Inorg. Chem.* **2005**, 2464. (g) Feyel, S.; Dobler, J.; Schröder, D.; Sauer, J.; Schwarz, H. *Angew. Chem., Int. Ed. Engl.* **2006**, *45*, 4681. (h) Feyel, S.; Schröder, D.; Rozanska, X.; Sauer, J.; Schwarz, H. *Angew. Chem., Int. Ed. Engl.* **2006**, *45*, 4677.

(30) Wang, X.; Neukermans, S.; Vanhoutte, F.; Janssens, E.; Verschoren, G.; Silverans, R. E.; Lievens, P. *Appl. Phys. B: Lasers Opt.* **2001**, *73*, 417.

(31) Fielicke, A.; Rademann, K. *Phys. Chem. Chem. Phys.* **2002**, *4*, 2621.

(32) Aubriet, F.; Muller, J. F. *J. Phys. Chem. A* **2002**, *106*, 6053.

(33) (a) Griffin, J. B.; Armentrout, P. B. *J. Chem. Phys.* **1997**, *106*, 4448. (b) Xu, J.; Rodgers, M. T.; Griffin, J. B.; Armentrout, P. B. *J. Chem. Phys.* **1998**, *108*, 9339. (c) Griffin, J. B.; Armentrout, P. B. *J. Chem. Phys.* **1998**, *108*, 8062. (d) Linton, C.; Simand, B.; Loock, H. P.; Wallin, S.; Rothschopf, G. K.; Gunion, R. F.; Morse, M. D.; Armentrout, P. B. *J. Chem. Phys.* **1999**, *111*, 2017. (e) Vardhan, D.; Liyanage, R.; Armentrout, P. B. *J. Chem. Phys.* **2003**, *119*, 4166. (f) Liu, F. Y.; Li, F. X.; Armentrout, P. B. *J. Chem. Phys.* **2005**, 123.

(34) Jackson, G. P.; King, F. L.; Goeringer, D. E.; Duckworth, D. C. *Int. J. Mass Spectrom.* **2002**, *216*, 85.

(35) (a) Chertihin, G. V.; Bare, W. D.; Andrews, L. *J. Chem. Phys.* **1997**, *107*, 2798. (b) Zhou, M. F.; Andrews, L. *J. Chem. Phys.* **1999**, *111*, 4230. (c) Andrews, L.; Rohrbacher, A.; Laperle, C. M.; Continetti, R. E. *J. Phys. Chem. A* **2000**, *104*, 8173.

(36) (a) Fan, J. W.; Wang, L. S. *J. Chem. Phys.* **1995**, *102*, 8714. (b) Wang, L. S.; Wu, H. B.; Desai, S. R. *Phys. Rev. Lett.* **1996**, *76*, 4853. (c) Wu, H. B.; Desai, S. R.; Wang, L. S. *J. Am. Chem. Soc.* **1996**, *118*, 7434. (d) Wang, Q.; Sun, Q.; Sakurai, M.; Yu, J. Z.; Gu, B. L.; Sumiyama, K.; Kawazoe, Y. *Phys. Rev. B* **1999**, *59*, 12672. (e) Gutsev, G. L.; Rao, B. K.; Jena, P.; Li, X.; Wang, L.-S. *J. Chem. Phys.* **2000**, *113*, 1473. (f) Sun, Q.; Sakurai, M.; Wang, Q.; Yu, J. Z.; Wang, G. H.; Sumiyama, K.; Kawazoe, Y. *Phys. Rev. B* **2000**, *62*, 8500. (g) Gutsev, G. L.; Jena, P.; Zhai, H.-J.; Wang, L.-S. *J. Chem. Phys.* **2001**, *115*, 7935. (h) Zhai, H.-J.; Wang, L.-S. *J. Chem. Phys.* **2002**, *117*, 7882. (i) Gutsev, G. L.; Bauschlicher, C. W., Jr.; Zhai, H.-J.; Wang, L.-S. *J. Chem. Phys.* **2003**, *119*, 11135. (j) Zhai, H.-J.; Kiran, B.; Cui, L.-F.; Li, X.; Dixon, D. A.; Wang, L.-S. *J. Am. Chem. Soc.* **2004**, *126*, 16134. (k) Zhai, H. J.; Wang, L.-S. *J. Chem. Phys.* **2006**, *125*, 164315. (l) Zhai, H. J.; Wang, L.-S. *J. Am. Chem. Soc.* **2007**, *129*, 3022.

(37) (a) Wenthold, P. G.; Jonas, K. L.; Lineberger, W. C. *J. Chem. Phys.* **1997**, *106*, 9961. (b) Ramond, T. M.; Davico, G. E.; Hellberg, F.; Svedberg, F.; Salen, P.; Soderqvist, P.; Lineberger, W. C. *J. Mol. Spectrosc.* **2002**, *216*, 1. (c) Ichino, T.; Gianola, A. J.; Andrews, D. H.; Lineberger, W. C. *J. Phys. Chem. A* **2004**, *108*, 11307.

(38) (a) Yang, D. S.; Hackett, P. A. *J. Elec. Spectros. Relat. Phenom.* **2000**, *106*, 153. (b) Yang, D. S. *Coord. Chem. Rev.* **2001**, *214*, 187.

(39) Green, S. M. E.; Alex, S.; Fleischer, N. L.; Millam, E. L.; Marcy, T. P.; Leopold, D. G. *J. Chem. Phys.* **2001**, *114*, 2653.

(40) (a) Pramann, A.; Nakamura, Y.; Nakajima, A.; Kaya, K. *J. Phys. Chem. A* **2001**, *105*, 7534. (b) Pramann, A.; Koyasu, K.; Nakajima, A.; Kaya, K. *J. Phys. Chem. A* **2002**, *106*, 4891. (c) Pramann, A.; Koyasu, K.; Nakajima, A.; Kaya, K. *J. Chem. Phys.* **2002**, *116*, 6521.

(41) Yoder, B. L.; Maze, J. T.; Raghavachari, K.; Jarrold, C. C. *J. Chem. Phys.* **2005**, *122*, 094313.

(42) Zhai, H.-J.; Dobler, J.; Sauer, J.; Wang, L.-S. *J. Am. Chem. Soc.* **2007**, *129*, 13270.

(43) (a) von Helden, G.; Kirilyuk, A.; van Heijnsbergen, D.; Sartakov, B.; Duncan, M. A.; Meijer, G. *Chem. Phys.* **2000**, *262*, 31. (b) van Heijnsbergen, D.; von Helden, G.; Meijer, G.; Duncan, M. A. *J. Chem. Phys.* **2002**, *116*, 2400. (c) van Heijnsbergen, D.; Demyk, K.; Duncan, M. A.; Meijer, G.; von Helden, G. *Phys. Chem. Chem. Phys.* **2003**, *5*, 2515.

(44) (a) Fielicke, A.; Meijer, G.; von Helden, G. *J. Am. Chem. Soc.* **2003**, *125*, 3659. (b) Fielicke, A.; Meijer, G.; von Helden, G. *Eur. Phys. J. D* **2003**, *24*, 69. (c) Fielicke, A.; Mitric, R.; Meijer, G.; Bonacic-Koutecky, V.; von Helden, G. *J. Am. Chem. Soc.* **2003**, *125*, 15716. (d) Demyk, K.; van Heijnsbergen, D.; von Helden, G.; Meijer, G. *Astron. Astrophys.* **2004**, *420*, 547.

(45) (a) Asmis, K. R.; Bruemmer, M.; Kaposta, C.; Santambrogio, G.; von Helden, G.; Meijer, G.; Rademann, K.; Wöste, L. *Phys. Chem. Chem. Phys.* **2002**, *4*, 1101. (b) Brummer, M.; Kaposta, C.; Santambrogio, G.; Asmis, K. R. *J. Chem. Phys.* **2003**, *119*, 12700. (c) Asmis, K. R.; Meijer, G.; Bruemmer, M.; Kaposta, C.; Santambrogio, G.; Wöste, L.; Sauer, J. *J. Chem. Phys.* **2004**, *120*, 6461. (d) Asmis, K. R.; Santambrogio, G.; Brummer, M.; Sauer, J. *Angew. Chem., Int. Ed. Engl.* **2005**, *44*, 3122. (e) Janssens, E.; Santambrogio, G.; Brummer, M.; Wöste, L.; Lievens, P.; Sauer, J.; Meijer, G.; Asmis, K. R. *Phys. Rev. Lett.* **2006**, 96.

(46) (a) Sambrano, J. R.; Andres, J.; Beltran, A.; Sensato, F.; Longo, E. *Chem. Phys. Lett.* **1998**, *287*, 620. (b) Calatayud, M.; Silvi, B.; Andres, J.; Beltran, A. *Chem. Phys. Lett.* **2001**, *333*, 493. (c) Calatayud, M.; Andres, J.; Beltran, A. *J. Phys. Chem. A* **2001**, *105*, 9760. (d) Sambrano, J. R.; Gracia, L.; Andres, J.; Berski, S.; Beltran, A. *J. Phys. Chem. A* **2004**, *108*, 10850. (e) Sambrano, J. R.; Andres, J.; Gracia, L.; Safont, V. S.; Beltran, A. *Chem. Phys. Lett.* **2004**, *384*, 56. (f) Gracia, L.; Andres, J.; Safont, V. S.; Beltran, A. *Organometallics* **2004**, *23*, 730.

(47) (a) Veliah, S.; Xiang, K. H.; Pandey, R.; Recio, J. M.; Newsam, J. M. *J. Phys. Chem. B* **1998**, *102*, 1126. (b) Xiang, K. H.; Pandey, R.; Recio, J. M.; Francisco, E.; Newsam, J. M. *J. Phys. Chem. A* **2000**, *104*, 990.

(48) (a) Reddy, B. V.; Khanna, S. N. *Phys. Rev. Lett.* **1999**, *83*, 3170. (b) Morisato, T.; Jones, N. O.; Khanna, S. N.; Kawazoe, Y. *Comput. Mater. Sci.* **2006**, *35*, 366.

(49) Chakrabarti, A.; Hermann, K.; Druzinic, R.; Witko, M.; Wagner, F.; Petersen, M. *Phys. Rev. B* **1999**, *59*, 10583.

(50) Zimmermann, R.; Steiner, P.; Claessen, R.; Reinert, F.; Hufner, S.; Blaha, P.; Dufek, P. *J. Phys.: Condens. Matter* **1999**, *11*, 1657.

(51) (a) Vyboishchikov, S. F.; Sauer, J. *J. Phys. Chem. A* **2000**, *104*, 10913. (b) Vyboishchikov, S. F.; Sauer, J. *J. Phys. Chem. A* **2001**, *105*, 8588. (c) Vyboishchikov, S. F. *J. Mol. Struc. Theochem.* **2005**, *723*, 53.

(52) Albaret, T.; Finocchi, F.; Noguera, C. *J. Chem. Phys.* **2000**, *113*, 2238.

(53) Gutsev, G. L.; Andrews, L.; Bauschlicher, C. W. *Theo. Chem. Accts.* **2003**, *109*, 298.

(54) Ayuela, A.; March, N. H.; Klein, D. J. *J. Phys. Chem. A* **2007**, *111*, 10162.

(55) (a) Guo, B. C.; Kerns, K. P.; Castleman, A. W. *Science* **1992**, *255*, 1411. (b) Guo, B. C.; Wei, S.; Purnell, J.; Buzza, S.; Castleman, A. W. *Science* **1992**, *256*, 515. (c) Cartier, S. F.; May, B. D.; Castleman, A. W. *J. Phys. Chem.* **1996**, *100*, 8175.

(56) (a) Pilgrim, J. S.; Duncan, M. A. *J. Am. Chem. Soc.* **1993**, *115*, 9724. (b) Pilgrim, J. S.; Duncan, M. A. *J. Am. Chem. Soc.* **1993**, *115*, 6958. (c) Duncan, M. A. *J. Cluster Sci.* **1997**, *8*, 239.

(57) Rohmer, M.-M.; Benard, M.; Poblet, J.-M. *Chem. Rev.* **2000**, *100*, 495.

(58) (a) van Heijnsbergen, D.; von Helden, G.; Duncan, M. A.; van Roij, A. J. A.; Meijer, G. *Phys. Rev. Lett.* **1999**, *83*, 4983. (b) von Helden, G.; van Heijnsbergen, D.; Meijer, G. *J. Phys. Chem. A* **2003**, *107*, 1671.

(59) (a) Gueorguiev, G. K.; Pacheco, J. M. *Phys. Rev. Lett.* **2002**, *88*, 115504. (b) Gueorguiev, G. K.; Pacheco, J. M. *Phys. Rev. B* **2003**, *68*, 241401.

(60) (a) Liu, P.; Rodriguez, J. A.; Hou, H.; Muckerman, J. T. *J. Chem. Phys.* **2003**, *118*, 7737. (b) Liu, P.; Rodriguez, J. A.; Muckerman, J. T. *J. Chem. Phys.* **2004**, *121*, 10321. (c) Liu, P.; Lightstone, J. M.; Patterson, M. J.; Rodriguez, J. A.; Muckerman, J. T.; White, M. G. *J. Phys. Chem. B* **2006**, *110*, 7449.

(61) (a) Varganov, S. A.; Gordon, M. S. *Chem. Phys.* **2006**, *326*, 97. (b) Varganov, S. A.; Dudley, T. J.; Gordon, M. S. *Chem. Phys. Lett.* **2006**, *429*, 49.

(62) Gutsev, G. L.; Andrews, L.; Bauschlicher, C. W. *Theo. Chem. Accts.* **2003**, *109*, 298.

(63) (a) *Clusters of Atoms and Molecules Vol. I*; Haberland, H., Ed.; Springer: Berlin, 1995. (b) *Clusters of Atoms and Molecules Vol. II*; Haberland, H., Ed.; Springer: Berlin, 1995..

(64) Johnston, R. L. *Atomic and Molecular Clusters*; Taylor & Francis: London, 2002.

(65) (a) Ticknor, B. W.; Duncan, M. A. *Chem. Phys. Lett.* **2005**, *405*, 214. (b) Jaeger, J. B.; Jaeger, T. D.; Duncan, M. A. *J. Phys. Chem. A* **2006**, *110*, 9310.

(66) Frisch, M. J. et al., *Gaussian 03 (Revision B.02)*; Gaussian, Inc.: Pittsburgh, PA, 2003.

(67) Becke, A. D. *J. Chem. Phys.* **1993**, *98*, 5648.

(68) Lee, C.; Yang, W.; Parr, R. G. *Phys. Rev. B* **1988**, *37*, 785.

(69) Perdew, J. R.; Chevary, J. A.; Vosko, S. H.; Jackson, K. A.; Pederson, M. R.; Singh, D. J.; Fiolhais, C. *Phys. Rev. B* **1992**, *46*, 6671.

(70) Dunning, T. H.; Hay, P. J. *Methods of Electronic Structure Theory*, Vol.2; Schaefer, H. F. ed.; Plenum Press: New York, 1977.

(71) (a) Hay, P. J.; Wadt, W. R. *J. Chem. Phys.* **1985**, *82*, 270. (b) Hay, P. J.; Wadt, W. R. *J. Chem. Phys.* **1985**, *82*, 284. (c) Hay, P. J.; Wadt, W. R. *J. Chem. Phys.* **1985**, *82*, 299.

(72) Cornett, D. S.; Peschke, M.; LaiHing, K.; Cheng, P. Y.; Willey, K. F.; Duncan, M. A. *Rev. Sci. Instrum.* **1992**, *63*, 2177.

(73) Sutton, L. E. *Table of interatomic distances and configuration in molecules and ions*, Supplement 1956−1959; Chemical Society: London, United Kingdom, 1965; special publication No. 18.

JP800588R